Chapter 6
Fatigue

6.1 Introduction to mechanical fatigue

Fatigue anslysis is an integral part of mechanical engineering design. In a narrow sense the term fatigue of materials and structual components means damage and fracture due to cyclic, repeateadly applied stress [1]. To understand fatigue process, knowledge from materials science [22, 14] and mechanics of solids [8, 9, 13, 16] is mandatory. A comprehensive compilation of different fatigue models is given in [20]. A probabilistic approach to fatigue can be found in [19].

Basically three stages can can be identified in the process of fatigue failure, cf. [7] and [22]: (i) nucleation and growth of micro-cracks and voids due to local inhomogeneities and local micro-plastic effects terminating in the creation of macro-cracks; (ii) stable crack propagation phase; (iii) unstable crack propagation phase leading to failure. In uniaxial fatigue tests the phase (ii) can further be divided into two stages: (a) crack growth on a plane of maximum shear and (b) crack propagation normal to the tensile stress.However, most of the fatigue life is spent in the stage (i). In contrast to the last two stages which are dominated by macro-cracks, the first stage is described by statistically distributed micromechanisms. Due to this characteristic, linear fracture mechanics cannot be applied in the first stage.

6.2 Multiaxial HCF models

In the high-cycle fatigue regime loading is proportional when the directions of the principal axes do not change.

In principle the HCF-models can be categorised in the following groups.

1. “Static” stress based criteria as Gough and Sines.
2. Critical plane models as proposed by Findley [4], Dang Van [2, 3], McDiarmid.
3. Criteria based on averaged stresses, i.e. integral approaches, proposed by Liu-Zenner [10], Papadopoulos [18].
4. Evolution equation based models first proposed by Ottosen et al. 2008 [17].

Figure 6.1: Illustration of the Findley criterion on the critical plane.

6.2.1 Findley's model

The basic idea of the Findley's HCF-model [4] is that fatigue fracture develops in a plane where the linear combination of the alternating shear stress and the normal stress appearing on that plane during the cycle attains its maximum. It can be formally written as

$$\max(\tau_{\mathrm{a},n} + k\sigma_n) = f, \tag{6.1}$$

where $\tau_{\mathrm{a},n}$ is the shear amplitude on a plane with a unit normal $\boldsymbol{n}$, i.e. $\tau_{\mathrm{a},n} = \Delta\tau_n/2$, and σ_n is the normal stress on the same plane. The two material parameters k and f can be determined from two fatigue loading tests, which can be for example

- alternating normal stress, $\sigma_{\mathrm{m}} = 0, \sigma_{\mathrm{af}} = \sigma_{\mathrm{a},R=-1}$,
- pulsating normal stress $\sigma_{\mathrm{m}} = \sigma_{\mathrm{a},R=0}$.

Other test combinations are also possible, like loading under alternating normal stress and alternating shear stress.

The idea of Findley's fatigue criterion on the critical plane is illustrated in Fig. 6.1.

6.2.1.1 *Example for determinig the parameters*

Determine the parameters k and f based on tests from alternating ($R = -1$) and pulsating ($R = 0$) normal stresses.

First, stresses in an arbitrary plane whose normal makes an angle θ to the loading direction. Then the unit normal vector $\boldsymbol{n}$ and the unit vector acting on the plane $\boldsymbol{s}$ have the forms

$$\boldsymbol{n} = \begin{pmatrix} \cos\theta \\ \sin\theta \end{pmatrix}, \qquad \boldsymbol{s} = \begin{pmatrix} \sin\theta \\ -\cos\theta \end{pmatrix} \tag{6.2}$$

and the normal stress and shear stress acting on the plane can be found from

$$\sigma_n = \boldsymbol{n}^T\boldsymbol{\sigma}\boldsymbol{n} = \sigma\cos^2\theta, \qquad \tau_n = \boldsymbol{n}^T\boldsymbol{\sigma}\boldsymbol{s} = \sigma\sin\theta\cos\theta. \tag{6.3}$$

Alternating normal stress. In this case the uniaxial normal stress in the direction of the loading can be expressed as $\sigma(t) = \sigma_{\mathrm{a}}\sin\omega t$ and thus in an arbitrary plane inclined by an angle θ from the loading direction

$$\sigma_n = \sigma_{\mathrm{a}}\cos^2\theta\sin\omega t, \tag{6.4}$$

$$\tau_n = \sigma_{\mathrm{a}}\sin\theta\cos\theta\sin\omega t. \tag{6.5}$$

Both the normal stress and shear stress attain their maximum at the same time. It is also observed that in this alternating loading case $\tau_{\mathrm{a},n} = \tau_n$, thus

$$\tau_{\mathrm{a},n} + k\sigma_n = \sigma_{\mathrm{a}}(\sin\theta\cos\theta + k\cos^2\theta) = f. \tag{6.6}$$

The maximum can be determined by investigating the function

$$g_{-1}(\theta) = \sin\theta\cos\theta + k\cos^2\theta. \tag{6.7}$$

The subscript -1 indicates that the function refers to the alternating loading case. For the existence of an extreme value of a function, the derivative has to vanish at the extremum point, therefore

$$\frac{\mathrm{d}g_{-1}}{\mathrm{d}\theta} = \cos^2\theta - \sin^2\theta - 2k\sin\theta\cos\theta = \cos 2\theta - k\sin 2\theta = 0, \tag{6.8}$$

giving the solution of the critical plane angle for the alternating loading case

$$\tan 2\theta_{-1} = \frac{1}{k}. \tag{6.9}$$

If the stress σ_a is at the fatigue limit, i.e. $\sigma_\mathrm{a} = \sigma_{-1}$, the value for the f parameter is obtained

$$f = \sigma_{-1}(\sin\theta_{-1}\cos\theta_{-1} + k\cos^2\theta_{-1}) = \sigma_{-1}\cos^2\theta_{-1}(\tan\theta_{-1} + k). \tag{6.10}$$

However, before calculating f, the value of k has to be known.

Pulsating normal stress. In the case of pulsating normal stress $\sigma_\mathrm{m} = \sigma_\mathrm{a}$ and the stress history can be written as $\sigma(t) = \sigma_\mathrm{a}(1-\cos\omega t)$. As in the case of atrenating normal stress, the shear stress and normal stress are in the same phase, thus attaing their maximum at the same time instant. Now the maximum normal stress is $\sigma_n = 2\sigma_a$ and $\tau_{\mathrm{a},n} = \sigma_\mathrm{a}$, thus

$$\tau_{\mathrm{a},n} + k\sigma_n = \sigma_\mathrm{a}(\sin\theta\cos\theta + 2k\cos^2\theta) = f. \tag{6.11}$$

Denoting the angle dependent term as $g_0(\theta) = \sin\theta\cos\theta + 2k\cos^2\theta$, the condition for the extremum is

$$\frac{\mathrm{d}g_0}{\mathrm{d}\theta} = \cos^2\theta - \sin^2\theta - 4k\sin\theta\cos\theta = \cos 2\theta - 2k\sin 2\theta = 0, \tag{6.12}$$

which gives the solution of the critical plane angle for the pulsating normal stress case

$$\tan 2\theta_0 = \frac{1}{2k}. \tag{6.13}$$

In both cases (6.6) and (6.11), the parameter f is the same on the critical planes, which gives the equality

$$\sigma_{-1}(\sin\theta_{-1}\cos\theta_{-1} + 2k\cos^2\theta_{-1}) = \sigma_0(\sin\theta_0\cos\theta_0 + 4k\cos^2\theta_0), \tag{6.14}$$

which can be also be written as

$$f = \sigma_{-1}\cos^2\theta_{-1}(\tan\theta_{-1} + 2k) = \sigma_0\cos^2\theta_0(\tan\theta_0 + 4k). \tag{6.15}$$

Terms depending on angles θ_{-1} and θ_0 can be eliminated using the equations (6.9) and (6.13).

For the elimination, the following trigonometric identities are usefull:

$$\tan\alpha = \frac{\tan 2\alpha}{1+\sqrt{1+\tan^2 2\alpha}}, \quad \text{and} \quad \cos^2\alpha = \frac{1}{1+\tan^2\alpha}. \tag{6.16}$$

For the alternating stress case

$$\tan\theta_{-1} = \frac{\tan 2\theta_{-1}}{1+\sqrt{1+\tan^2 2\theta_{-1}}} = \frac{1/k}{1+\sqrt{1+1/k^2}} = \frac{1}{k+\sqrt{1+k^2}}, \tag{6.17}$$

$$\cos^2\theta_{-1} = \frac{1}{1+\tan^2\theta_{-1}} = \frac{(k+\sqrt{1+k^2})^2}{1+(k+\sqrt{1+k^2})^2}. \tag{6.18}$$

Thus

$$f = \sigma_{-1}\cos^2\theta_{-1}(\tan\theta_{-1} + k) = \tfrac{1}{2}\sigma_{-1}(k+\sqrt{1+k^2}). \tag{6.19}$$

Alternatively for the pulsating case, it is obtained

$$\tan\theta_0 = \frac{\tan 2\theta_0}{1+\sqrt{1+\tan^2 2\theta_0}} = \frac{1/2k}{1+\sqrt{1+1/(2k)^2}} = \frac{1}{2k+\sqrt{1+(2k)^2}}, \tag{6.20}$$

$$\cos^2\theta_0 = \frac{1}{1+\tan^2\theta_0} = \frac{(2k+\sqrt{1+(2k)^2})^2}{1+(2k+\sqrt{1+(2k)^2})^2}. \tag{6.21}$$

Therefore

$$f = \sigma_0\cos^2\theta_0(\tan\theta_0 + 2k) = \tfrac{1}{2}\sigma_0(2k+\sqrt{1+(2k)^2}). \tag{6.22}$$

Finally from (6.15), an equation

$$\frac{\sigma_{\mathrm{a},R=0}}{\sigma_{\mathrm{a},R=-1}} = \frac{\sigma_0}{\sigma_{-1}} = \frac{k+\sqrt{1+k^2}}{2k+\sqrt{1+(2k)^2}} \tag{6.23}$$

is obtained. Denoting the fatigue stress ratio $\sigma_0/\sigma_{-1} = \xi$, the parameter k can be found as a function of the ratio ξ as

$$k = \frac{\frac{1}{2}(1-\xi^2)}{\sqrt{\xi(5\xi-2-2\xi^2)}}. \tag{6.24}$$

A typical range of value for metals is $0.2 \leq k \leq 0.3$. Notice that when $\xi \downarrow 1/2$ then $k \to \infty$. When $\xi = 0.5$ the pulsating and that the mean normal stress has no effect on

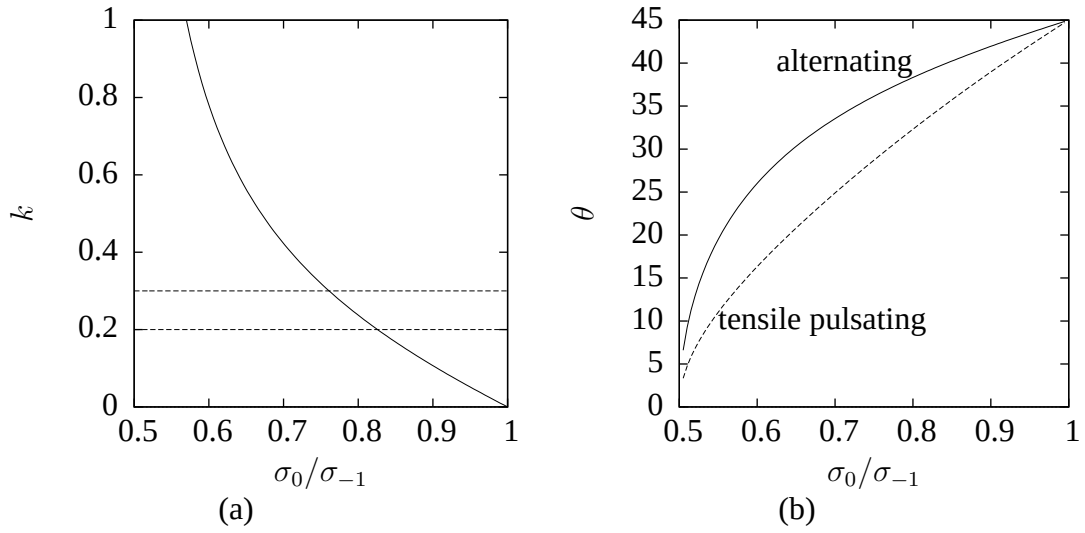

Figure 6.2: Findley's fatigue criterion. (a) Material parameter k as a function of the fatigue stress ratio and (b) the angle of the critical plane in alternating and in tensile pulsating normal stress states.

the fatigue limit, which is unrealistic. In the Haigh diagram this means that the fatigue limit is a horizontal line. The value of k as a function of the fatigue stress ratio σ_0/σ_{-1} is shown in Fig.6.2a. In addition the critical plane angles in both alternating and pulsating tensile normal stresses as a function of the fatigue stress ratio are shown in Fig. 6.2b.

The parameter f can be obtained either from (6.19) or (6.22), i.e.

$$f = \tfrac{1}{2}\sigma_{-1}(k + \sqrt{1+k^2}) = \tfrac{1}{2}\sigma_0(2k + \sqrt{+(2k)^2}). \tag{6.25}$$

It can be shown that the f-parameter can be given also using the fatigue stress amplitude in pure shear stress as

$$f = \sqrt{1+k^2}\ \tau_{-1}, \tag{6.26}$$

where τ_{-1} is the shear fatigue stress in alternating shear test. Derivation of this result is left as an exercise for an interested reader. The ratio between alternating shear and normal stress fatigue limits predicted by the Findley's model is therefore

$$\frac{\tau_{-1}}{\sigma_{-1}} = \frac{k + \sqrt{1+k^2}}{2\sqrt{1+k^2}}. \tag{6.27}$$

This relationship is shown in Fig. 6.3 as a function f the σ_0/σ_{-1} ratio.

The Findley model can also be used for finite life analysis. In this case the f-parameter is replaced by

$$f = \sqrt{1+k^2}\ \tau_{-1}N^b, \tag{6.28}$$

where N is the number of cycles and b is an additional material parameter.

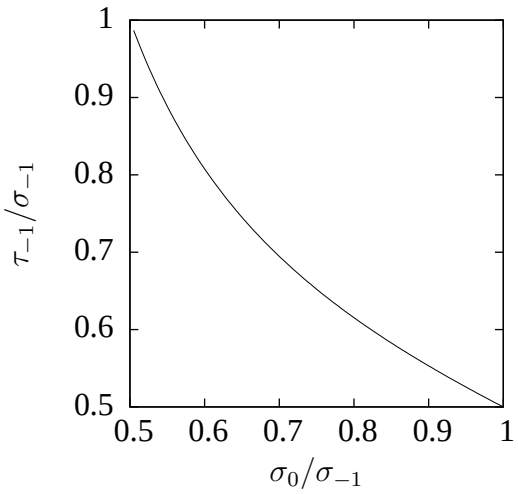

Figure 6.3: Alternating shear stress fatigue limit as a function of the fatigue stress ratio σ_0/σ_{-1} according to the Findley fatigue criterion.

6.2.2 Dang Van's model

Dang Van's criterion [2, 3] is based on a two-scale approach. In metals the fatigue crack initiates at the grain level in the so-called persistent slip bands (PSB) due to alternating shear stresses. The tensile micro-scale hydrostatic stress will open the crack and accelerate its growth along the PSB. The macroscale stresses which appear in the macroscale equilibrium equations are denoted as $\boldsymbol{S}$ and the micro-scale stresses appearing in the grains are denoted as $\boldsymbol{\sigma}$. The criterion for fatigue is postulated in the micro-scale as

$$\tau(t) + a\sigma_{\mathrm{h}}(t) = b, \tag{6.29}$$

where $\tau(t)$ and $\sigma_{\mathrm{h}}(t)$ are the instantaneous shear and hydrostatic stresses on the slip band. If $\tau(t) + a\sigma_{\mathrm{h}}(t) < b$, $\forall t$ the structure will elastically shake-down to the applied loading.

The macro- and microscale stresses are related as

$$\boldsymbol{\sigma}(t) = \boldsymbol{S}(t) + \operatorname{dev} \boldsymbol{\rho}, \tag{6.30}$$

where $\boldsymbol{\rho}$ is the stabilised residual stress tensor. During the elastic shakedown the microscale yield surface will expand and move according to isotropic and kinematic hardening laws and the stabilized residual stress tensor $\boldsymbol{\rho}$ designates the distance from the center of the yield surcafe from the origin. The state of shakedown is found if the stress path is completely inside the expanded and displaced yield surface. On the meridia plane the situation is illustrated in Fig. 6.4.

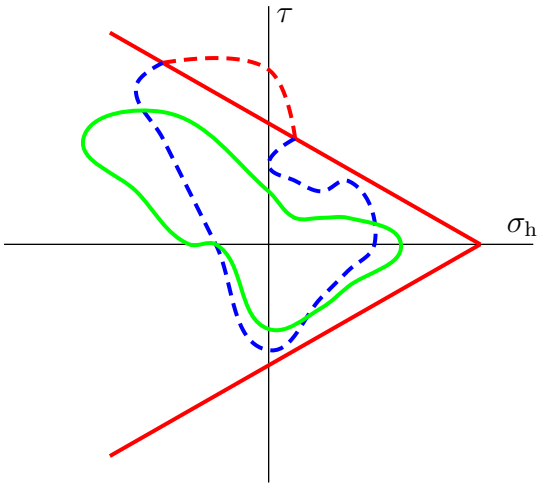

Figure 6.4: Dang Van fatigue failure criterion in the meridian plane of the micro-stress. Safe stress path shown by solid green line and stress path resulting to fatigue fracture by a dashed blue/red line.

In proportional loading the residual stress tensor $\boldsymbol{\rho}$ can be computed from the opposite value of the average of two extreme macroscopic stress tensors

$$\boldsymbol{\rho} = -\frac{1}{2}\left(\boldsymbol{S}(t_1) + \boldsymbol{S}(t_2)\right) \tag{6.31}$$

where t_1 and t_2 designates the two time instants at which the extreme values of the macroscopic stress $\boldsymbol{S}$ is obtained.

6.2.2.1 Example for determining the parameters

The use of Dang Van's fatigue criterion is illustrated first by determining the two material parameters a and b from alternating ($R = -1$) and pulstating tensile ($R = 0$) normal stress fatigue tests with amplitude values σ_{-1} and σ_0, respectively. Since the macroscopic stress tensor is uniaxial, it has the form

$$\boldsymbol{S} = \begin{pmatrix} S_{11} & 0 & 0 \\ 0 & 0 & 0 \\ 0 & 0 & 0 \end{pmatrix}. \tag{6.32}$$

In the alternating stress case at the fatigue limit the stress S_{11} is given as

$$S_{11} = \sigma_{-1} \sin \omega t, \tag{6.33}$$

and in the pulsating tensile stress case

$$S_{11} = \sigma_0 (1 - \cos \omega t). \tag{6.34}$$

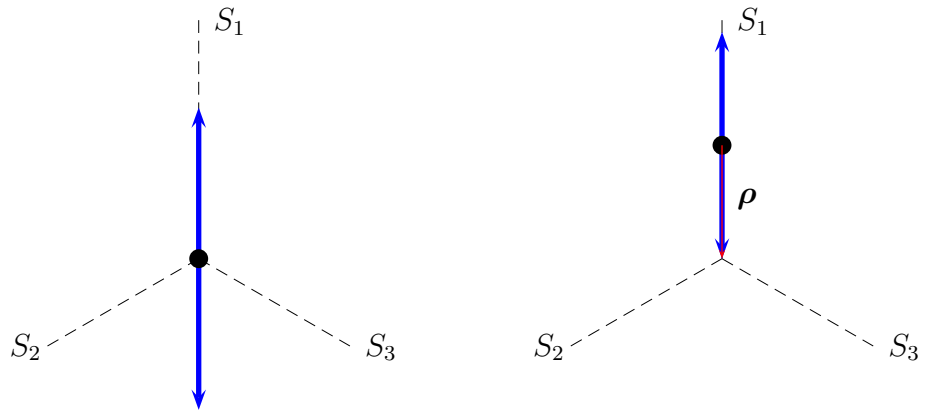

Figure 6.5: Cyclic (a) alternating stress state and (b) tensile pulsating stress state in the macroscopic stress principal stress space.

Both of these cyclic stress paths are illustarated in the principal stress space in Fig. 6.5.

It is clear that the stabilized residual stress tensor vanish in the alternating uniaxial notrmal stress state and in the uniaxial pulsating tensile stress state it has only one nonzero element ρ_{11}.

In the alternating uniaxial normal stress state the maximum shear stress is $\tau_{\max} = \frac{1}{2}\sigma_{-1}$ and the hydrostatic stress at the same time instant is $\sigma_{\mathrm{h}} = \frac{1}{3}\sigma_{-1}$. Thus, at the fatigue limit the following equation has to be satisfied

$$\tfrac{1}{2}\sigma_{-1} + a\tfrac{1}{3}\sigma_{-1} = b. \tag{6.35}$$

In the tensile pulsating uniaxial stress state the component ρ_{11} is clearly the mean macroscopic stress $-S_{11,\mathrm{m}}$. It can also be deduced from (6.31) where

$$\boldsymbol{S}(t_1) = \boldsymbol{0}, \quad \text{and} \quad \boldsymbol{S}(t_2) = \begin{pmatrix} 2\sigma_0 & 0 & 0 \\ 0 & 0 & 0 \\ 0 & 0 & 0 \end{pmatrix}, \quad \text{thus} \quad \boldsymbol{\rho} = -\begin{pmatrix} \sigma_0 & 0 & 0 \\ 0 & 0 & 0 \\ 0 & 0 & 0 \end{pmatrix}. \tag{6.36}$$

Deviatoric part of the stabilised residual stress tensor is

$$\operatorname{dev}\boldsymbol{\rho} = \begin{pmatrix} -\frac{2}{3}\sigma_0 & 0 & 0 \\ 0 & \frac{1}{3}\sigma_0 & 0 \\ 0 & 0 & \frac{1}{3}\sigma_0 \end{pmatrix}, \tag{6.37}$$

and the micro-stress tensor is

$$\boldsymbol{\sigma}(t) = \boldsymbol{S}(t) + \operatorname{dev}\boldsymbol{\rho} = \begin{pmatrix} \frac{1}{3}\sigma_0 - \sigma_0\cos\omega t & 0 & 0 \\ 0 & \frac{1}{3}\sigma_0 & 0 \\ 0 & 0 & \frac{1}{3}\sigma_0 \end{pmatrix}. \tag{6.38}$$

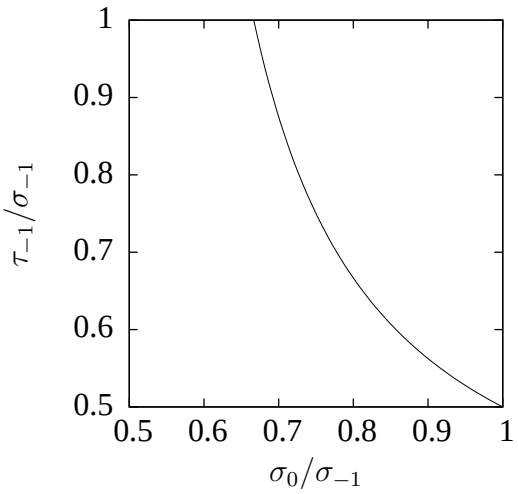

Figure 6.6: Alternating shear stress fatigue limit as a function of the fatigue stress ratio σ_0/σ_{-1} according to the Dang Van fatigue criterion.

The maximum shear stress and hydrostatic stresses have expressions

$$\tau_{\max} = \tfrac{1}{2}\sigma_0|\cos\omega t|, \quad \text{and} \quad \sigma_{\mathrm{h}} = \tfrac{1}{3}\operatorname{tr}\boldsymbol{\sigma} = \tfrac{1}{3}\sigma_0(1-\cos\omega t), \tag{6.39}$$

and the most dangerous maximum values occur at the same time instant and are $\max\tau_{\max} = \frac{1}{2}\sigma_0$ and $\max\sigma_{\mathrm{h}} = \frac{2}{3}\sigma_0$. Therefore inserting these values to the fatigue criterion (6.29), gives

$$\tfrac{1}{2}\sigma_0 + a\tfrac{2}{3}\sigma_{-1} = b. \tag{6.40}$$

Putting together (6.35) and (6.40), the a coefficient can be solved, resulting in expression

$$a = \frac{3(1-\sigma_0/\sigma_{-1})}{2(2\sigma_0/\sigma_{-1}-1)} = \frac{3(1-\xi)}{2(2\xi-1)}. \tag{6.41}$$

Then, the b parameter can be solved either from (6.35) or (6.40), giving

$$b = \frac{\sigma_0}{2(2\sigma_0/\sigma_{-1}-1)} = \frac{\sigma_0}{2(2\xi-1)} = \frac{\xi\sigma_{-1}}{2(2\xi-1)}. \tag{6.42}$$

It can be noticed that the b parameter equals with the alternating shear fatigue limit τ_{-1}. Dependency of alternating shear fatigue stress on the fatigue stress ratio σ_0/σ_{-1} is shown in Fig. 6.6.

The cyclic uniaxial stress states in the medidian plane of the microtress is illustrated in Fig. 6.7.

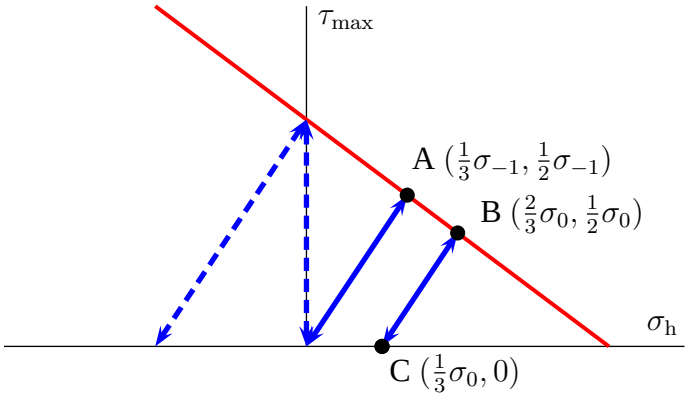

Figure 6.7: Determining the material parameters using the Dang Van criterion. Fatigue limit is shown by a red line and the uniaxial loading cases by blue lines. To fix the failure line two tests have to be conducted. In the text the failure line is determined from alternating and tensile pulsating normal stress tests, which are shown by blue solid lines and the fatigue stresses from tests as solid black circles, points A and B. Alternative uniaxial tests are alternating shear and compressive pulsating tests shown by blue dashed lines. Notice that the meridian plane is for the microstress.

.

6.2.3 Evolution equation based fatigue model

An appealing model for high-cycle fatigue was proposed by Ottosen et al. [17]. In their approach the concept of a moving endurance surface in the stress space is postulated together with a damage evolution equation. Movement of the endurance surface is modelled with a deviatoric tensor which defines the center of the endurance surface in a similar way than the back-stress tensor in plasticity, thus memorizing the load history. Damage evolution is activated whenever the stress state is outside the endurance domain defined by the endurance surface and the time rate of the endurance surface is positive. In this model uniaxial and multiaxial stress states are treated in a unified manner for arbitrary loading histories, thus avoiding cycle-counting techniques.

It is well known that the endurance limits of a material change with load conditions and that loading within these limits do not result in damage develoment. Based on this feature Ottosen et al. postulated an endurance surface β in the stress space as

$$\beta = (\bar{\sigma} + AI_1 + \sigma_{-1})/\sigma_{-1} = 0, \tag{6.43}$$

where A is a positive nondimensional material parameter, which in uniaxial cycling loading between $\sigma_{\mathrm{m}} - \sigma_{\mathrm{a}}$ and $\sigma_{\mathrm{m}} + \sigma_{\mathrm{a}}$ can be associated as the slope of the Haigh-diagram, and σ_{-1} is the endurance limit for alternating stress, see also Fig. 6.8. Denoting the stress tensor as $\boldsymbol{\sigma}$, the first stress invariant is $I_1 = \mathrm{tr}\,\boldsymbol{\sigma}$, the effective stress is defined in terms of

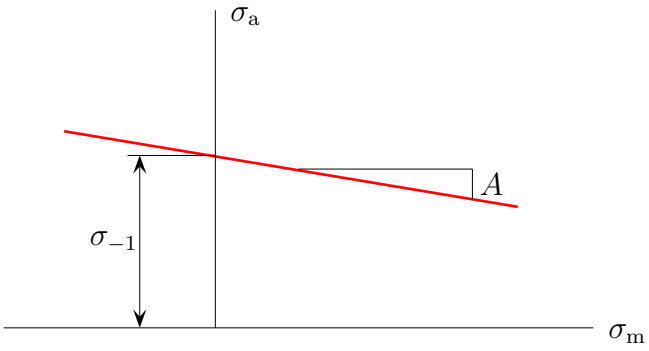

Figure 6.8: Haigh-diagram.

the second invariant of the reduced deviatoric stress $\boldsymbol{s} - \boldsymbol{\alpha}$ as

$$\bar{\sigma} = \sqrt{3J_2(\boldsymbol{s} - \boldsymbol{\alpha})} = \sqrt{\tfrac{3}{2}(\boldsymbol{s} - \boldsymbol{\alpha}) : (\boldsymbol{s} - \boldsymbol{\alpha})}, \tag{6.44}$$

where $\boldsymbol{s} = \boldsymbol{\sigma} - \frac{1}{3}\,\mathrm{tr}(\boldsymbol{\sigma})\boldsymbol{I}$ is the deviatoric stress tensor. Shape of the endurance surface in the deviatoric plane is circular and the meridian planes are straight lines as in the case of the Drucker-Prager model in plasticity. The center point in the deviatoric plane is defined by the $\boldsymbol{\alpha}$-tensor, which memorizes the load history.

The slope in the Haigh diagram A can be determined if the fatigue stress in tensile pulsating loading is known as

$$A = \frac{\sigma_{-1} - \sigma_0}{\sigma_0}. \tag{6.45}$$

For the evolution of the deviatoric back-stress tensor $\boldsymbol{\alpha}$, a hardening rule similar to Ziegler's kinematic hardening rule in plasticity theory is adopted

$$\dot{\boldsymbol{\alpha}} = C(\boldsymbol{s} - \boldsymbol{\alpha})\dot{\beta}, \tag{6.46}$$

where C is a non-dimensional material parameter and the dot denotes the time rate. Evolution of the back-stress (6.46) and damage (6.48) takes place only if the following conditions are satisfied

$$\beta \geq 0, \quad \text{and} \quad \dot{\beta} \geq 0, \tag{6.47}$$

which mean that damage accumulation can only occur when the stress is moving away from the endurance surface. In contrast to plasticity, the stress state can lie outside the endurance surface. The idea for the endurance surface movement is illustrated in Fig. 6.9.

Material damage is described with a scalar variable $D \in [0, 1]$, for which the evolution is governed by equation of the form

$$\dot{D} = g(\beta, D)\dot{\beta}. \tag{6.48}$$

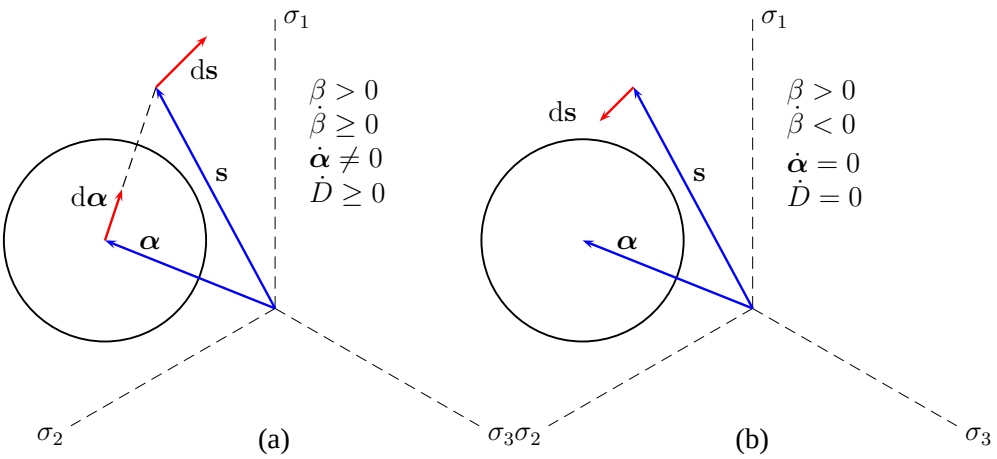

Figure 6.9: Ottosen's HCF model. (a) Movement of the endurance surface and damage growth when the stress is outside the endurance surface and moving away from it. (b) When the stress is outside the endurance surface, damage and back stress does not evolve.

Ottosen et al. [17] choose a simple exponential form for the damage evolution law

$$\dot{D} = K \exp(L\beta)\dot{\beta}. \tag{6.49}$$

6.2.4 Comparison of methods

Bibliography

[1] V.V. Bolotin. *Mechanics of Fatigue*. CRC Mechanical Engineering Series. CRC Press, Boca Raton, 1999.

[2] K. Dang Van. Macro-micro approach in high-cycle multiaxial fatigue. In D.L. McDowell, editor, *Advances in Multiaxial Fatigue*, number 1191 in ASTM STP, pages 120–130, Philadelphia, 1993. Americal Society for Testing and Materials.

[3] K. Dang Van, G. Gailletaud, G. Flavenot, A. Le Douaron, and H.P. Lieurade. Criterion for high cycle fatigue failure under multiaxial loading. In M.W. Brown and K.J. Miller, editors, *Biaxial and Multiaxial Fatigue*, number 3 in EGF, pages 459–478, London, 1989. Mechanical Engineering Publications.

[4] W.N. Findley. A theory for the effect of mean stress on fatigue of metals under combined torsion and axial load or bending. *Journal of Engineering for Industry*, pages 301–306, November 1959.

[5] W. Flügge. *Viscoelasticity*. Blaisdell Publishing Company, 1967.

[6] G.A. Holzapfel. *Nonlinear Solid Mechanics - A Continuum Approach for Engineering*. John Wiley & Sons, 2000.

[7] J. Lemaitre. How to use damage mechanics. *Nuclear Engineering and Design*, 80(2):233–245, 1984.

[8] J. Lemaitre and J.-L. Chaboche. *Mechanics of Solid Materials*. Cambridge University Press, 1990.

[9] J. Lemaitre and R. Desmorat. *Engineering Damage Mechanics, Ductile, Creep, Fatigue and Brittle Failures*. Springer-Verlag, Berlin, Heidelberg, 2005.

[10] J. Liu and H. Zenner. Fatigue limut of ductile metals under multiadial loading. In A Carpinteri, M. de Freitas, and A. Spagnoli, editors, *Biaxial/multiaxial fatigue and fracture*, pages 147–163. Elsevier Science Ltd. and ESIS, 2003.

[11] J. Lubliner. *Plasticity Theory*. Pearson Education, Inc., 1990.

[12] L.E. Malvern. *Introduction to the Mechanics of a Continuous Medium*. Prentice Hall, Englewood Cliffs, New Jersey, 1969.

[13] S. Murakami. *Continuum Damage Mechanics*, volume 185 of *Solid Mechanics and Its Applications*. Springer Netherlands, 2012.

[14] Y. Murakami. *Metal Fatigue, Effects of Small defects and Nonmetallic Inclusions*. Elsevier Science, 2002.

[15] S. Nemat-Nasser and M. Hori. *Micromechanics: Overall Properties of Heterogeneous Materials*, volume 37 of *North-Holland series in Applied Mathematics and Mechanics*. North-Holland, 1993.

[16] N.S. Ottosen and M. Ristinmaa. *The Mechanics of Constitutive Modeling*. Elsevier, 2005.

[17] N.S. Ottosen, R. Stenström, and M. Ristinmaa. Continuum approach to high-cycle fatigue modeling. *International Journal of Fatigue*, 30(6):996–1006, June 2008.

[18] I. V. Papadopoulos. Long life fatigue under multiaxial loading. *International Journal of Fatigue*, 23(10):839 – 849, 2001.

[19] R. Rabb. *Todennäköisyysteoriaan pohjautuva väsymisanalyysi*. BoD - Books on Demand, Helsinki, Finland, 2013.

[20] D.F. Socie and G.B. Marquis. *Multiaxial Fatigue*. Society of Automotive Engineers, Inc., Warrendale, Pa, 2000.

[21] A.J.M. Spencer. *Continuum Mechanics*. Dover Publications, Inc., 2004. First published by Longman Group UK Limited in 1980.

[22] S. Suresh. *Fatigue of Materials*. Cambridge University Press, 2nd edition, 1998.